

# Model-based method to anticipate Hopf bifurcation

Jules Malavieille, Master Sea sciences

Internship supervised by Jean-Christophe Poggiale from June 2 to July 11, 2025

## Table des matières

<b>1</b>	<b>Abstract</b>	<b>1</b>
<b>2</b>	<b>Introduction</b>	<b>1</b>
<b>3</b>	<b>Matérials and method</b>	<b>1</b>
3.1	Models . . . . .	1
3.2	Log-likelihood . . . . .	2
3.3	D-statistic and Probability Distribution . . . . .	2
3.4	Algorithm . . . . .	3
3.5	Data . . . . .	3
<b>4</b>	<b>Results</b>	<b>4</b>
4.1	Test of the algorithm . . . . .	4
4.2	Validation of the algorithm with simulated Hopf bifurcation . . . . .	4
4.3	Detection of a Hopf bifurcation . . . . .	5
<b>5</b>	<b>Discussion</b>	<b>6</b>
5.1	Test without bifurcation . . . . .	6
5.2	Sensitivity of $\sigma$ . . . . .	6
5.3	Limitations and perspectives . . . . .	6
<b>6</b>	<b>Conclusion</b>	<b>7</b>
<b>7</b>	<b>Bibliographie</b>	<b>7</b>

# 1 Abstract

A Hopf bifurcation corresponds to the transition from a stable state to an oscillatory regime. This type of behavior occurs in many fields : biology, ecology, epidemiology, mechanics, chemistry, economics, and more. We have adapted the method of Boettiger and Hastings (2012), which is based on comparing two models—with and without bifurcation—using a statistic called the D-statistic and its associated ROC curve, to the case of Hopf bifurcations. The algorithm showed promising effectiveness, but it was only tested on a very limited amount of simulated data. To evaluate its robustness and improve it, it must be tested on a larger set of simulated data and time series, while also improving the model's sensitivity to noise intensity. Nonetheless, this approach paves the way for broader developments toward the generalized detection of other types of critical transitions triggered by bifurcations of an underlying dynamical system.

# 2 Introduction

When a system transitions from a stable focus to an unstable one, giving rise to a limit cycle and thus an oscillatory behavior, this phenomenon is called a Hopf bifurcation (Y.A. Kuznetsov, 1994).

Such bifurcations are found across many disciplines : in epidemiology, with the seasonality of epidemics (V. Ecle-rova et al., 2015) ; in microbiology, with bacterial cultures under certain conditions (L. Xiaofang et al., 2009) ; in mechanics, with instabilities in thermoacoustic engines (S. Mondal et al., 2018) ; in ecology, with predator-prey dynamics and the paradox of enrichment (G.F. Fussman et al., 2000) ; in chemistry, with oscillatory reactions such as the Belousov-Zhabotinsky reaction (R.J. Field, R.M. Noyes, 1974) ; and in socio-economics, with macroeconomic cycles (Q. Jao, J. Ma, 2009).

However, although the theoretical principles and consequences of such bifurcations are well understood, the early detection of oscillatory regimes remains a relatively unexplored topic. From a time series, is it possible to anticipate the emergence of Hopf bifurcations ? What conditions must these time series meet ? To what extent are such bifurcations detectable ? To address these ques-

tions, the method of Boettiger and Hastings (2012) is generalized. This method was originally developed for fold bifurcations.

# 3 Matériaux and method

## 3.1 Models

To model a bifurcation following the approach of Boettiger and Hastings (2012), it is necessary to use the normal form corresponding to the bifurcation under consideration. In the case of the Hopf bifurcation, the polar coordinates of the normal form (Y.A. Kuznetsov, 1994) are described as follows :

$$\frac{dr}{dt} = \mu r - r^3 \quad (1)$$

$$\frac{d\psi}{dt} = 1 \quad (2)$$

where  $r$  represents the amplitude of the oscillating signal,  $\mu$  is the control parameter of stability, and  $\phi$  is the phase angle of the system, assumed to be decoupled from the dynamics of  $r$  (Y.A. Kuznetsov, 1994). Analyzing the equilibrium points of this equation gives :

$$\begin{aligned} \frac{dr}{dt} &= 0 \\ \mu r - r^3 &= 0 \\ r^* &= 0 \quad \text{or} \quad r^* = \sqrt{\mu} \quad \text{if } \mu > 0 \end{aligned}$$

We then deduce that if  $\mu < 0$ , the only equilibrium point is  $r = 0$ , which is stable. Thus, there are no oscillations. Conversely, if  $\mu > 0$ , then  $r = 0$  becomes unstable and a limit cycle with amplitude  $r = \sqrt{\mu}$  emerges.

To represent a real system in which a Hopf bifurcation gradually appears over time, we assume that  $\mu$  varies linearly with time such that :  $\mu = \mu_0 + mt$ , where  $\mu_0 < 0$ ,  $t$  is time, and  $m$  is the forcing rate of  $\mu$ . We assume  $m > 0$  and small enough so that over short time intervals,  $\mu$  is approximately constant, justifying the use of equations (1) and (2). We deduce that since  $\mu$  increases, the amplitude of the data increases as it follows  $r = \sqrt{\mu}$ . This increase in amplitude reveals the transition to an oscillatory regime.

Following the method of Boettiger and Hastings (2012), we define  $\phi$  as the equilibrium point of the normal form such that :  $\phi = 0$  if  $\mu < 0$  and  $\phi = \sqrt{\mu}$  if  $\mu > 0$ .

We then define the test model representing amplitude dynamics around  $\phi$  as :

$$dX = \sqrt{\mu}(\phi - X), dt + \sigma\sqrt{\phi}, dB \quad (3)$$

where  $X$  represents the simulated amplitude,  $\sigma$  is the noise intensity, and  $dB$  is white noise. This model drives  $X$  toward the attractor  $\phi$ , whether in the stable case ( $\phi = 0$ ) or in the presence of a limit cycle ( $\phi = \sqrt{\mu}$ ). In parallel, we define the null model (or reference model), constructed such that it remains stable ( $\phi = 0$ ) for all  $t$ . It is incapable of simulating a bifurcation :

$$dX = (-X\mu_0), dt + \sigma, dB \quad (4)$$

This model follows a linear dynamic around 0 with constant noise. Since  $m$  does not vary in this model, we have  $\mu = \mu_0$ , so  $\phi = 0$ . The system therefore never bifurcates.

### 3.2 Log-likelihood

In order to compare the null model (NM) and the test model (TM), we use a log-likelihood approach, as proposed by C. Boettiger and A. Hastings (2012) and formalized by Gardiner (1983). This method relies on comparing the observed data with the simulated trajectories of each model. To do so, we begin by characterizing the average behavior of each of the two models. The null model, which is linear around  $X = 0$ , has the following expected value and variance :

$$\begin{aligned} E(x_i, |, NM) &= 0 \\ V(x_i, |, NM) &= \frac{\sigma^2}{2\mu_0}(1 - e^{-2\mu t}) \end{aligned}$$

The expected value and variance of the test model depend on time through the dynamics of  $\phi$  and therefore of  $\mu$ .

$$\begin{aligned} \frac{dE}{dt}(x_i, |, TM) &= 2\sqrt{\mu}(\phi - E) \\ \frac{dV}{dt}(x_i, |, TM) &= -2\sqrt{\mu}V + \sigma^2\phi \end{aligned}$$

where  $E$  and  $V$  respectively denote the expectation and variance of  $X(t)$ . We integrate these equations numerically using the Milstein scheme (J. Higham, 2001) to determine  $E$  and  $V$  at each time  $t$ .

We can then compute the log-likelihood of each point  $x_i$  under the assumption of a normal distribution :

$$\begin{aligned} w &= \frac{t_i}{t_{max}} \\ L(x_i) &= w \left( -\frac{1}{2} \log(2\pi) - \log(\sqrt{V}) - \frac{1}{2} \frac{(x_i - E)^2}{V} \right) \end{aligned}$$

$w$  is a time-dependent weight, giving more importance to observations close to the bifurcation point. This enhances the test's sensitivity to amplitude increases (T. Ueno et al., 2012).

The total log-likelihood is then computed as :

$$\log V = - \sum L(x_i) + \frac{1}{m} \quad (5)$$

The term  $L(x_i)$  represents the "standard" log-likelihood, and the term  $\frac{1}{m}$  is a penalty inversely proportional to  $m$ . This prevents artificially adjusting  $m$  toward zero due to a likelihood plateau, which would make detection trivial and the model incorrect (Q. Song, F. Liang, 2015). This log-likelihood measures the mismatch between observed data and a simulated model with given parameters. Therefore, it can be used to calibrate the model's parameters. Among all tested parameter combinations, we seek the one that minimizes the total log-likelihood. This combination provides the best fit of the model to the observed data.

### 3.3 D-statistic and Probability Distribution

Once the optimal parameters of the test model and the null model are determined, we retain the associated log-likelihoods. We then compare the quality of each model using a comparison statistic, the D-statistic (J.P. Huelssenbeck, J.J. Bull, 1996), defined as :

$$Dstat = 2(\log V(NM) - \log V(TM))$$

This metric expresses to what extent the data deviate from the null hypothesis (absence of bifurcation) in favor of the test model (presence of a Hopf bifurcation).

By simulating a large number of time series from the null model and the test model, we can compute two sets of D-statistics, respectively under the null hypothesis and under the bifurcation hypothesis.

We can then estimate the probability distributions of these D-statistics using a kernel density estimation (KDE) with a Gaussian kernel (Y.C. Chen, 2017; L. Wasserman, 2006), defined as :

$$f(Dstat) = \frac{1}{nh} \sum \mathcal{N}\left(\frac{x - Dstat}{h}, 1\right) \quad (6)$$

$f(Dstat)$  is the estimated probability density function of the D-statistic values,  $h$  is the smoothing bandwidth determined via cross-validation (A.W. Bowman, 1984),  $\mathcal{N}(\mu, \sigma)$  is a normal distribution with mean  $\mu$  and variance  $\sigma$ ,  $n$  is the number of values to estimate,  $x$  is the set of x-values over which we estimate the density, and  $Dstat$  is the set of D-statistic values whose distribution we wish to estimate.

### 3.4 Algorithm

The method relies on an algorithm designed to detect the onset of a Hopf bifurcation from a noisy time series. The general algorithm is presented in Figure 1.

**Step 1 : Extraction of oscillation amplitude** From the raw time series, we extract the oscillation amplitude using a peak-to-peak interpolation (A. Pikovsky et al., 2001). We identify the maxima and minima of the series and compute the absolute difference between each pair of successive extrema. A spline interpolation is then applied to these absolute differences to obtain a continuous amplitude function (L. Wasserman, 2006; P. Sablonnière, 2005).

**Step 2 : Estimation of the test model parameters** Using the extracted amplitude, we estimate the parameters of the test model by minimizing the previously defined log-likelihood. This allows us to determine the optimal values of  $\mu$  and  $m$  that describe the amplitude trajectory under the Hopf bifurcation hypothesis. Note that  $\sigma$  is estimated independently from  $\mu$  and  $m$  using a Monte Carlo method (see Section 5.2).

**Step 3 : Simulation generation** Using the estimated parameters, we generate 100 simulations of the test model and 100 simulations of the null model by numerically integrating the equations presented in Section 3.1 using the Milstein scheme (J. Higham, 2001).

**Step 4 : D-statistic computation** For each simulated trajectory, we compute the log-likelihood under both models and calculate the corresponding D-statistic. This

process is applied to both null model data (under the stability hypothesis) and test model data (under the bifurcation hypothesis). We thus obtain two distributions of D-statistics : one for “stability” and one for “bifurcation.”

**Step 5 : Estimation of probability densities** Using kernel density estimation (KDE) with a Gaussian kernel, we estimate the probability density functions of the “stability” and “bifurcation” D-statistic distributions.

**Step 6 : ROC curve** From these two distributions, we compute the ROC (Receiver Operating Characteristic) curve (T. Fawcett, 2006). This curve plots the true positive rate against the false positive rate across different decision thresholds. It evaluates the ability of a test to distinguish between two hypotheses. A diagonal curve indicates a poor test (equal rate of true and false positives), while a logarithmic or rectangular shape indicates a good test (more true than false positives).

**Step 7 : AUC computation** To obtain a more precise and quantifiable performance measure than the shape of the ROC curve, we compute the AUC (Area Under the Curve), which corresponds to the integral of the ROC curve between 0 and 1 (J. Muschelli, 2021). The AUC ranges from 0.5 (random test) to 1 (perfect test). The closer the AUC is to 1, the more effective the test.

### 3.5 Data

To evaluate the algorithm, it is useful to generate simulated time series in which a Hopf bifurcation is known, controlled, and reproducible. This allows us to know *a priori* whether a bifurcation is present or not, while generating a large number of different datasets. To this end, we use a stochastic version of the Rosenzweig-MacArthur model (Rosenzweig and MacArthur, 1963)(Gardiner, 1983). This model describes a predator-prey interaction with logistic growth of the prey and a saturating functional response of the predator. White noise is added to capture the inherent uncertainty in models simulating realistic data :

$$\begin{aligned} dx &= \left( rx \left( 1 - \frac{x}{K} \right) - \frac{axy}{b+x} \right) dt + \sigma dB_x \\ dy &= \left( \frac{eaxy}{b+x} - my \right) dt + \sigma dB_y \end{aligned}$$

Here,  $x(t)$  is the prey density over time,  $y(t)$  is

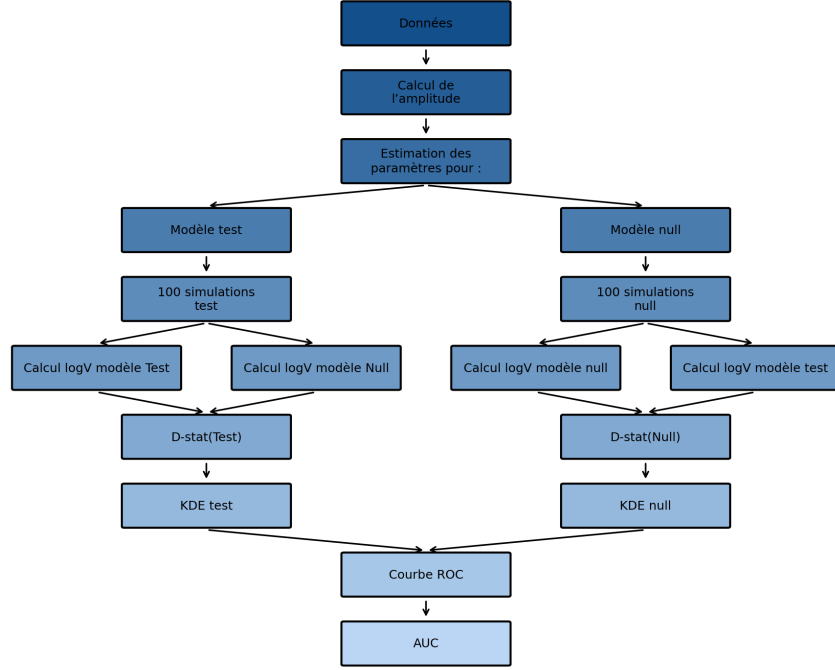


FIGURE 1 – Algorithm used to detect Hopf bifurcation, adapted from C. Boettiger and A. Hastings (2012)

the predator density,  $r$  is the intrinsic growth rate of the prey,  $K$  is the environmental carrying capacity,  $a$  is the predation rate of  $x$  by  $y$ ,  $b$  is the half-saturation constant,  $e$  is the conversion efficiency from prey to predator, and  $m$  is the mortality rate of the predator.  $dB_x$  and  $dB_y$  represent white noise affecting  $x$  and  $y$  respectively.

The parameters are fixed as follows :  $r = 1.2$ ,  $a = 0.5$ ,  $b = 0.5$ ,  $e = 0.7$ ,  $m = 0.2$ , and  $\sigma = 0.01$ . The parameter  $K$  varies linearly over time according to  $K_{n+1} = K_n + 0.0019dt$ , with  $K_0 = 0.5$ . This linear change in  $K$  induces a transition from a stable state to an oscillatory regime via a Hopf bifurcation.

The model is numerically integrated using the Milstein scheme (J.Higham, 2001) over 1000 time steps with 100,000 values. It produces time series similar to Figure 2.

Incorporating stochastic dynamics is essential, as it allows amplitude to increase before the bifurcation point due to the decreasing strength of the restoring force toward the stable equilibrium. The noise thus naturally generates small oscillations prior to the bifurcation. This is what enables the algorithm to detect early warning signs of the regime shift.

## 4 Results

### 4.1 Test of the algorithm

### 4.2 Validation of the algorithm with simulated Hopf bifurcation

To validate the algorithm's functionality, we first verify whether it is capable of detecting a Hopf bifurcation when it is indeed present. For this, we simulate the test model using arbitrary but realistic parameters. In this example, we set  $\mu_0 = -10$  and  $m = 0.23$ , ensuring a long stable period followed by a clear transition to a limit cycle.

From this simulated dataset, we apply the log-likelihood minimization procedure to estimate the optimal parameters for both the null and test models. The goal is then to compare the trajectories of the two models against the observed data.

As shown in Figure 3, the test model and its expected value accurately capture the simulated data. This indicates that the test model successfully detects the transition from a stable state to an oscillatory regime. In contrast, the null model, which cannot represent

## Proie du modèle de Ronsenzweig-McArthur

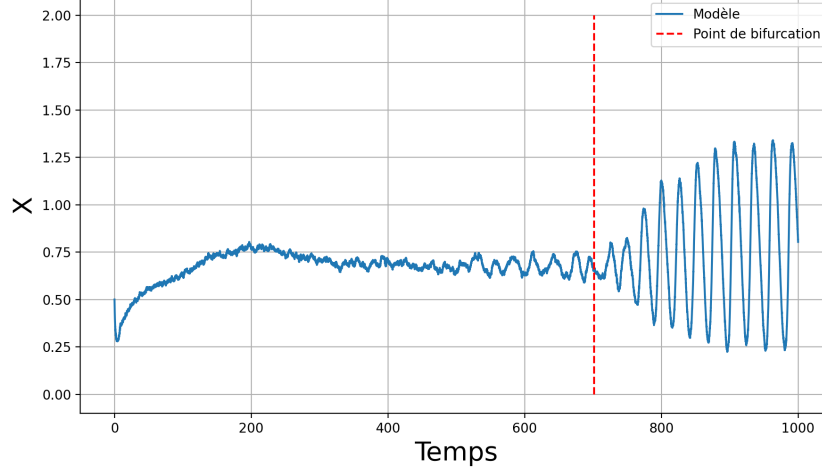


FIGURE 2 – Simulation of prey density in a stochastic Rosenzweig-MacArthur model

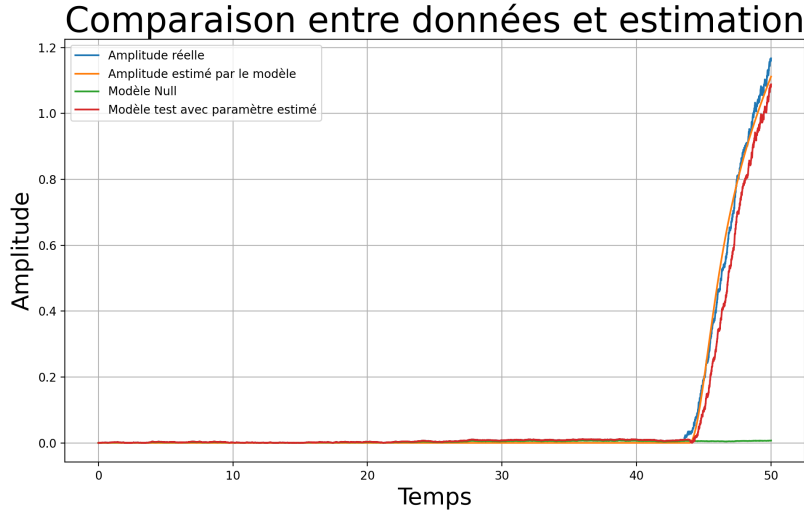


FIGURE 3 – Amplitude over time for the simulated data (blue), expected value (orange), null model (green), and test model (red), all calibrated with parameters optimized via log-likelihood

bifurcations, fails to explain the transition and remains centered around zero.

### 4.3 Detection of a Hopf bifurcation

To anticipate a bifurcation before it occurs, we apply the algorithm to a truncated version of the dataset from Figure 2, keeping only the data prior to the bifurcation point.

We then run the full algorithm on these partial data : parameter estimation, simulation generation, computation of D-statistics, and estimation of the probability densities via Gaussian KDE. Figure 4 (left) shows

the resulting distributions.

We observe a clear separation between the two probability laws. This suggests a strong distinction between the null model and the test model, indicating that a bifurcation is being captured by the test model based on the observed data. This is confirmed by the ROC curve (Figure 4, right), which yields an AUC of 0.97, corresponding to 97% true positives. The system thus predicts an upcoming Hopf bifurcation.

This demonstrates that the algorithm is capable of detecting, from pre-bifurcation amplitude data, an approaching Hopf bifurcation. It is therefore a viable tool for forecasting transitions to oscillatory regimes.

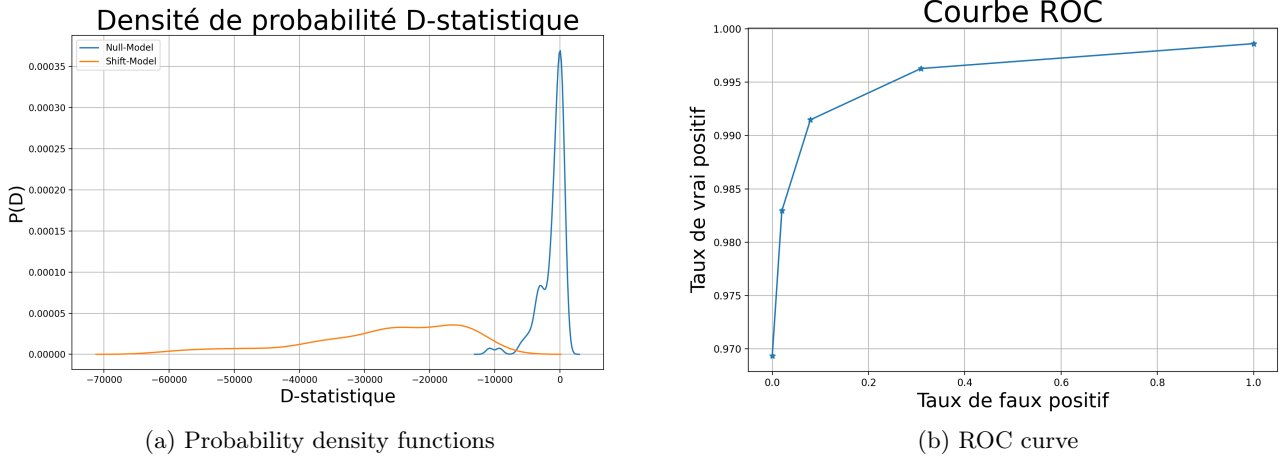


FIGURE 4 – Estimated probability distributions of D-statistics under the null hypothesis (blue) and the bifurcation hypothesis (orange) (left). Associated ROC curve (right).

## 5 Discussion

### 5.1 Test without bifurcation

To ensure that the algorithm does not produce false positives, it is important to test it on data that does not include any transition to an oscillatory regime, but instead remains in a purely stable state. To do so, we fix  $K$  at  $K_0 = 0.5$ , which prevents any Hopf bifurcation from occurring.

We then reapply the exact same algorithm as before. The resulting ROC curve is nearly linear (see Figure 5), indicating that the test does not distinguish between the two hypotheses—stability and bifurcation—in these data. It therefore fails to reject the null hypothesis of stability in a truly stable dataset.

This behavior is expected for a statistical test : in the absence of signal, the ROC curve remains close to the diagonal (T. Fawcett, 2006). This demonstrates that the method does not produce false positives.

### 5.2 Sensitivity of $\sigma$

The parameter  $\sigma$ , which controls the intensity of the stochastic noise, cannot be directly optimized by minimizing the log-likelihood between the data and the test model. Indeed, since the extracted amplitude is completely smooth, it does not reflect any noisy structure. Therefore, estimating the noise intensity is initially irrelevant. However, there is always some discrepancy, however small, between the data and the test model. This

discrepancy can be considered as uncertainty around the model's precision. To better adapt the model to the data, we can incorporate noise explicitly.

To find the optimal value of  $\sigma$ , we use a Monte Carlo simulation-based optimization method that minimizes the log-likelihood (P.E. Kloeden, 1992 ; C.G. Robert and G. Casella, 2002). The method consists in generating  $n$  simulations of the test model for a given value of  $\sigma$ , then computing the mean and variance at each time point  $t$  using these  $n$  simulations. These estimates are then plugged into the standard log-likelihood calculation (without penalty or weighting). The optimal  $\sigma$  is the one that minimizes this log-likelihood. This procedure introduces a coherent noisy structure into the model, without overpowering its deterministic dynamics.

### 5.3 Limitations and perspectives

To strengthen the robustness of this model, it is essential to confront it with a wider variety of scenarios. This includes both testing it on other dynamical systems exhibiting Hopf bifurcations and applying it to real-world time series showing transitions from stable states to oscillatory regimes.

Moreover, the methodology itself can be improved in multiple ways. For instance, it could be combined with early-warning signal methods or even extended into a hybrid model by incorporating machine learning components.

Finally, this algorithm could be generalized to detect



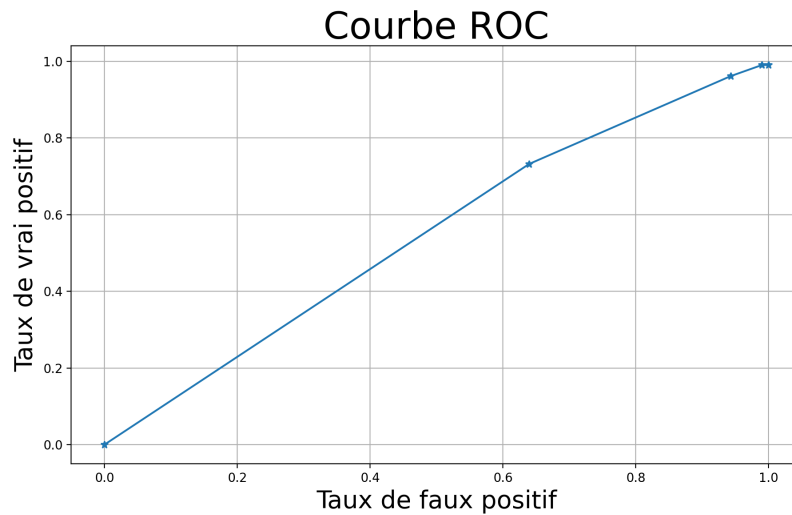


FIGURE 5 – ROC curve for a stable system without bifurcation

other types of regime shifts by adapting the normal form to match the expected bifurcation type. This would allow the creation of a generic detection algorithm tailored to various dynamical transitions.

## 6 Conclusion

The algorithm presented here demonstrates a strong ability to detect Hopf bifurcations on simulated data. To confirm its validity, it should be further tested on real datasets as well as on different models exhibiting Hopf bifurcations to enhance its robustness and generalization. This work thus provides a promising model-based framework for detecting Hopf bifurcations and lays the groundwork for broader developments in the early prediction of bifurcations in complex systems.

## 7 Bibliographie

### Références

- [1] Boettiger, C. , Hastings, A.(2012). Quantifying limits to detection of early warning for critical transitions, *Journal of the royal society*, Vol 9, 2527-2539. doi :10.1098/rsif.2012.0125
- [2] Bowman, A.W. (1984). An alternative method of cross-validation for the smoothing of density estimates, *Biometrika*, Vol 71(2), 353-360.
- [3] Chen, Y.C. (2017). A tutotial on kernel density estimation and recent advances, *Biostatistics & epidemiology*, <https://doi.org/10.48550/arXiv.1704.03924>
- [4] Fawcett, T. (2006), An introduction to ROC analysis, *Pattern Recognition Letters*, Vol 27(8), 861-874. <https://doi.org/10.1016/j.patrec.2005.10.010>
- [5] Field, J.R., Noyes, R.M. (1974), Oscillation in chemical system.IV.limit cycle behaviour in a model of a real chemical reaction, *The Journal of Chemicals Physics*, Vol 60(5), 1877-1884. <https://doi.org/10.1063/1.1681288>
- [6] Fussman, G.F. (2000), Crossing the Hopf bifurcation in a live predator-prey system, *Science*, Vol 290(5495), 1358-1360. DOI 10.1126/science.290.5495.1358
- [7] Gao, Q., Ma, J. (2009), Chaos and Hopf bifurcation of a finance system, *Nonlinear Dynamics*, Vol 58, 209-216. DOI 10.1007/s11071-009-9472-5
- [8] Gardiner, C.W. (1983). *Handbook of stochastic methods for physics, chemistry and natural sciences* (1983), Springer

- [9] Higham, J. (2001). An algorithmic introduction to numerical simulation of stochastic differential equations, *Siam review*, Vol 43(3), 525-546. <http://www.jstor.org/stable/3649798>
- [10] Huelsenbeck, J.P., Bull, J.J. (1996). A likelihood ratio test to detect conflicting phylogenetic signal, *Systematic biology*, Vol 45(1), 92-98. DOI : 10.1093/sysbio/45.1.92
- [11] Kloeden, P.E., Platen, E. (1992). *Numerical solution of stochastic differential equations* (1992), Springer
- [12] Kuznetsov, Y.A. (1994). *Elements of applied bifurcation theory* (1994), Springer
- [13] Mondal, S. et al. (2019). Early detection of thermoacoustic instabilities using hidden Markov model, *Combustion science and technology*, Vol 191(8), 1309-1336. <https://doi.org/10.1080/00102202.2018.1523900>
- [14] Muschelli, J. (2020). ROC and AUC with a binary predictor : a potentially misleading metric, *Health and Human Services*, Vol 37(3), 696-708. doi :10.1007/s00357-019-09345-1.
- [15] Pikovsky, A. et al. (2001). *Synchronization, a universal concept in nonlinear sciences* (2001), Cambridge
- [16] Robert, C.P., Casella, G. (2002). *Monte Carlo statistical methods* (2002), Springer
- [17] Sablonnière, P. (2005) *Univariate spline quasi interpolant and application to numerical analysis*. <https://doi.org/10.48550/arXiv.math/0504022>
- [18] Song, Q., Liang, F. (2015). A Split-and-Merge Bayesian Variable Selection Approach for Ultrahigh Dimensional Regression *Journal of the royal scociety*. Vol 77, 947-972. <https://doi.org/10.1111/rssb.12095>
- [19] Ueno, T. et al. (2012). Weighted Likelihood Policy Search with Model Selection, *Neural computation*, Vol 26(2), 349-376
- [20] Wasserman, L. (2006). *All of non-parametric statistics* (2006), Springer
- [21] Xiaofang, L. et al. (2008). Stability and Hopf bifurcation of a delay differential system in microbial continuous culture, *Internation Journal of Biomathematics*, Vol 2(03), 321-328. <https://doi.org/10.1142/S179352450900073X>